Electronic Supplementary Material (ESI) for Physical Chemistry Chemical Physics.
This journal is © the Owner Societies 2024

Supporting Information: Turing Patterns on Rotating Spiral Growing Domains

Leonardo Silva-Dias,[†,‡] Irving R. Epstein,[*,†] and Milos Dolnik[†]

†*Department of Chemistry and Center for Complex Systems, MS015, Brandeis University, Waltham, Massachusetts 02454-9110, USA*

‡*Department of Chemistry, Federal University of Sao Carlos , Sao Carlos, Sao Paulo 13.565-905, Brazil*

E-mail: epstein@brandeis.edu

Introduction

We present in this document animations of Turing pattern formation in rotating spiral growing domains from experiments and simulations, as well as, a simplified parametric diagram $\dot{\mathbf{r}} \times n$ with $r_0 = \lambda_T$. Therefore, the supporting information is organized as follows: in the sections "Experimental Turing pattern growth" and "Simulated Turing patterns" we show the animations of all experiments and simulations presented in the main paper, respectively. In the section "Parametric diagram with $r_0 = \lambda_T$", we depict the simplified diagram.

Experimental Turing pattern growth

The animations display experimental data of the spiral growth process and Turing pattern formation, summarized in Figure 2 of the main text. Such animations were constructed using images taken 10 minutes apart, and the frame rate is 4 fps.

- animation-2A.avi - It shows the pattern formation displayed in Figure 2A, i.e., $n = 0.88$, ($\dot{\mathbf{r}}_E = 0.2$ mm/h, $\dot{\theta}_E = 3.0^o$/min.).

- animation-2B.avi - It shows the pattern formation displayed in Figure 2B, i.e., $n = 2.22$, ($\dot{\mathbf{r}}_E = 0.5$ mm/h, $\dot{\theta}_E = 3.0^o$/min.).

- animation-2C.avi - It shows the pattern formation displayed in Figure 2C, i.e., $n = 3.55$, ($\dot{\mathbf{r}}_E = 0.4$ mm/h, $\dot{\theta}_E = 1.5^o$/min.).

Simulated Turing patterns

The animations display simulated data of the spiral growth process and Turing pattern formation, summarized in Figures 3, 5, and 6 of the main text. Such animations were constructed using images taken 5 time units apart, and the frame rate is 4 fps.

- animation-3A.avi - It shows the pattern formation displayed in Figure 3A, i.e., $n = 0.88$, ($\dot{\mathbf{r}}_T = 5.37 \times 10^{-2}$ su/tu, $\dot{\theta}_T = 3.0^o$/tu.).

- animation-3B.avi - It shows the pattern formation displayed in Figure 3B, i.e., $n = 2.22$, ($\dot{\mathbf{r}}_T = 0.134$ su/tu, $\dot{\theta}_T = 3.0^o$/tu.).

- animation-3C.avi - It shows the pattern formation displayed in Figure 3C, i.e., $n = 3.55$, ($\dot{\mathbf{r}}_T = 0.107$ su/tu, $\dot{\theta}_T = 1.5^o$/tu.).

- animation-5A.avi - It shows the pattern formation displayed in Figure 5A, i.e., $n = 0.5$, ($\dot{\mathbf{r}}_T = 0.242$ su/tu, $\dot{\theta}_T = 24.0^o$/tu.).

- animation-5B.avi - It shows the pattern formation displayed in Figure 5B, i.e., $n = 1.55$, ($\dot{\mathbf{r}}_T = 8.05 \times 10^{-2}$ su/tu, $\dot{\theta}_T = 2.58^o$/tu.).

- animation-5C.avi - It shows the pattern formation displayed in Figure 5C, i.e., $n = 2.6$, ($\dot{\mathbf{r}}_T = 0.107$ su/tu, $\dot{\theta}_T = 2.05^o$/tu.).

- animation-5D.avi - It shows the pattern formation displayed in Figure 5D, i.e., $n = 3.6$, ($\dot{\mathbf{r}}_T = 0.161$ su/tu, $\dot{\theta}_T = 2.22^o$/tu.).

- animation-6A.avi - It shows the pattern formation displayed in Figure 6A, i.e., $n = 2.66$, ($\dot{\mathbf{r}}_T = 0.107$ su/tu, $\dot{\theta}_T = 1.99^o$/tu.), and $r_0 = 2.0$ su.

- animation-6B.avi - It shows the pattern formation displayed in Figure 6B, i.e., $n = 2.66$, ($\dot{\mathbf{r}}_T = 0.107$ su/tu, $\dot{\theta}_T = 1.99^o$/tu.), and $r_0 = 10.0$ su.

Parametric diagram with $r_0 = \lambda_T$

In this section, we present a summarized parametric diagram of $\dot{\mathbf{r}} \times n$ with an initial nucleation site equal to $r_0 = \lambda_T$ in Figure 1. Differently from what is exposed in Figure 4B, the regions of double and triple spirals shift to the left, centralizing around $n = 2$ and $n = 3$. This confirms our initial supposition about the relationship between n and the most probable spiral multiplicity, and also it shows that the final morphologies have a strong dependence on the initial size of the nucleation site.

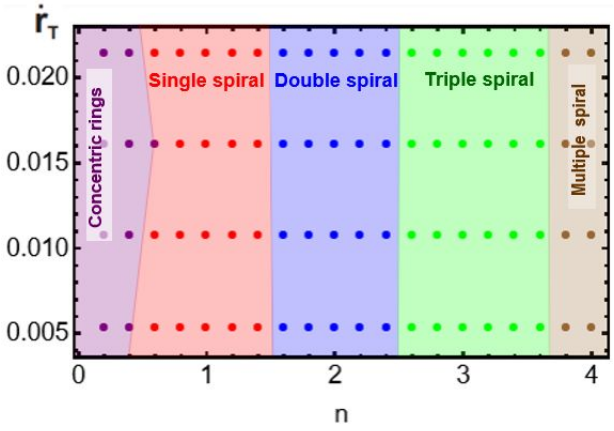

Figure S1: Parametric diagrams $\dot{\mathbf{r}}_T \times n$ with $r_0 = \lambda_T$, representing regions of concentric rings, single spirals, double spirals, triple spirals, multiple spirals, and transitional structures (black dots) observed in numerical simulations with the Lengyel-Epstein model. Each dot in the diagrams represents the result of a single simulation.